A Convex Optimization Framework for Dynamic Balancing of Planar Linkages

B. Demeulenaere, J. Swevers, J. De Schutter
K.U.Leuven, Department of Mechanical Engineering,
Celestijnenlaan 300 B, B-3001, Heverlee, Belgium
bram.demeulenaere@mech.kuleuven.ac.be

Abstract

This paper focusses on reducing the dynamic reactions (shaking force, shaking moment and driving torque) of plane, crank-rocker four-bars through counterweight addition. Determining the mass parameters of the counterweights constitutes an optimization problem, which is classically considered to be nonlinear and hence difficult to solve. A first contribution of this paper is the proof that this optimization problem can be reformulated as a *convex* program, that is, a nonlinear optimization problem that still has a unique (and hence guaranteed *global*) optimum, which can be found with great efficiency. Because of the unique features of this formulation, it becomes possible to investigate (and by the guarantee of obtaining a global optimum, in fact *prove*) the ultimate limits of dynamic balancing, in a reasonable amount of time. When applied to a particular example, this results in design charts, which clearly illustrate (i) the tradeoff between minimizing the different dynamic reactions, and (ii) the fact that adding counterweights is effective, but at the cost of a significant amount of added mass. These design charts constitute a second contribution of the present work.

1 Introduction

Dynamic balancing is the art of reducing (or eliminating) the *dynamic reactions*, involved with the rotary-to-oscillating motion conversion, imposed by a mechanism. The dynamic reactions, considered here, are (i) the *shaking force* transmitted to the supporting frame, (ii) the *shaking moment* transmitted to the frame and (iii) the input or driving torque, required to drive the mechanism with constant drive speed. The motivation for dynamic balancing is twofold. Firstly, the shaking moment and shaking force cause vibrations of the frame (which in turn cause noise, wear, fatigue, . . .), and should therefore be minimized. Secondly, highly peaked input torques necessitate large flywheels (compromising the machine's start/stop behavior) or high actuator torques (and hence a large motor) in order to obtain a (nearly) constant drive speed.

Spring addition and counterweight addition constitute two prominent dynamic balancing approaches. This paper focusses on counterweight addition for dynamically balancing (or for short, *counterweight balancing, CWB*) plane, crank-rocker four-bar mechanisms. An elaborate literature survey of CWB is not given here. The newcomer in the field is referred to the essential paper [1] and the comprehensive survey [2].

It is well-known, see e.g. [3, 4, 5] that CWB involves a tradeoff between minimizing the different dynamic reactions. Therefore, determining the counterweights' mass parameters inherently constitutes an optimization problem. A major contribution of this paper is the proof that this optimization problem, which is in general considered to be 'nonlinear' and hence difficult to solve, can be reformulated as a *convex* optimization problem, that is, a nonlinear optimization problem with a unique (and hence guaranteed *global*) optimum, which can be found with great efficiency. These features induce a second contribution, that is, the development, for the case of a plane, crank-rocker four-bar, of design charts, which clearly illustrate the aforementioned tradeoff, and provide as such an extension of [4].

The paper is organized as follows. First an introduction to convex optimization is given (Section 2). Section 3 develops the CWB optimization problem in its original, nonconvex form. After that, it is shown in Section 4 how this problem is reformulated as an equivalent, convex optimization problem. This convex formulation is subsequently used to construct the aforementioned design charts (Section 5). Section 6 finally discusses the obtained results.

2 A convex optimization primer

In fact, the great watershed in optimization isn't between linearity and nonlinearity, but between convexity and nonconvexity. [6]. The first part of this citation expresses a common misconception among engineers: if either the goal function or the constraints of an optimization problem are nonlinear, the problem is difficult to solve. Indeed, *linear programs*, that is, optimization problems with a goal function and constraints that are linear in the optimization variables, have nice properties: there exist effective algorithms that can reliably solve (that is, determine the *global* optimum) even large problems, with hundreds or thousands of variables and constraints. However, many engineers consider 'linear' and 'easy' on the one hand, and 'nonlinear' and 'difficult' on the other hand, as being synonyms in the area of optimization.

This is not quite true, as suggested by the second part of Rockafellar's citation: *convex programs* (CPs) are *nonlinear* optimization problems, for which very effective algorithms exist that can reliably and efficiently determine the *global* optimum, even for large problems. As with linear programming, it can be said, with only a bit of exaggeration, that, if a problem can be formulated as a convex program, the original problem has been solved [7]. Formulating an optimization problem as a CP, therefore, has great advantages.

Unfortunately, recognizing convex optimization problems, or those that can be transformed into CPs, is not straightforward: the art and challenge in convex optimization is in problem *formulation*. Once a problem is formulated as a convex program, it is relatively straightforward to solve it. In dealing with nonlinear programs (that is, nonlinear optimization problems that are not, or can't be proven to be, convex), things are reversed: formulating the optimization problem is mostly relatively straightforward. Here, however, the art and challenge is in *solving* the optimization problem. This involves testing different optimization algorithms, tuning the parameters of the chosen optimization algorithm (this can itself be an optimization problem), developing a methodology to produce a good enough initial guess,... Examples of such papers in the area of CWB are e.g. [5] and [8].

At the moment, the two most prominent application areas of convex optimization are control theory and combinatorial optimization, whereas the number of applications in mechanical engineering is rather limited. Two well-known overview papers mention only two applications: structural optimization [9] and optimization of robot grasping force [10].

Several classes of CPs exist, each of which are a subclass of a more general type of problems. Starting with the smallest class, we have: linear programs (LPs), convex quadratic programs (QPs), second-order cone programs (SOCPs) and semidefinite programs (SDPs): LP $\subset$ QP $\subset$ SOCP $\subset$ SDP $\subset$ CP.

SOCPs are of particular interest here. In an SOCP, one minimizes a linear goal function, subject to linear equality constraints, linear inequality constraints and *second-order cone* constraints [7]. The latter constraints are of the general form: $\|A \cdot x + b\| \leq c^T x + d$, where $x \in \mathbb{R}^n$ is the optimization variable, and $A \in \mathbb{R}^{k \times n}$, $b \in \mathbb{R}^k$, $c \in \mathbb{R}^n$ and $d \in \mathbb{R}$ constitute problem data. $\| \cdot \|$ denotes the $L2$-norm: $\|x\| = \sqrt{x^T \cdot x}$. From here on, vectors and matrices are denoted using bold characters, as opposed to scalars.

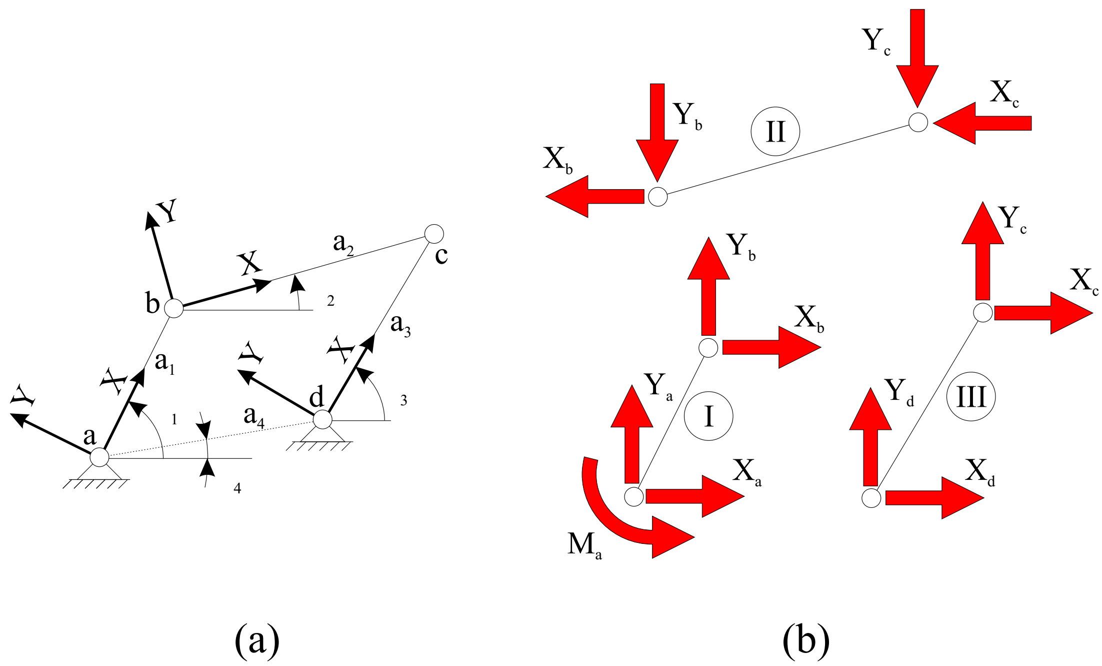

Figure 1: Kinematic scheme (a) and free-body diagram (b) of a plane, crank-rocker four-bar mechanism.

3 Original optimization problem

3.1 Definition of dynamic reactions

Figure $1(a)$ shows the kinematic scheme of a plane, crank-rocker four-bar. Link I, the crank, is assumed to rotate at constant speed. The time in which the crank makes one complete revolution determines the mechanism's period of motion T [s]. Link II, the coupler, connects the crank with link III, the rocker. The latter performs an oscillating (rocking) motion. a_{i} [m], $i = \{1, 2, 3, 4\}$ denote the link lengths, while $\phi_{\text{i}}(t)$ [rad], $i = \{1, 2, 3\}$ are the link angles. ϕ_4 [rad] is a fixed angle, which is of no importance if gravity is neglected. This classical assumption in the area of high-speed linkages is also made here.

Figure $1(b)$ shows a free-body diagram, based on which the dynamic reactions are defined. The x and y-component of the shaking force F_{shak} [N], acting on the machine frame, respectively equal:

$$F_{\text{shak,x}} = -\left(X_{\text{a}} + X_{\text{d}}\right); \quad F_{\text{shak,y}} = -\left(Y_{\text{a}} + Y_{\text{d}}\right).$$

The shaking moment M_{shak} [N-m] w.r.t. the point a equals:

$$M_{\text{shak}} = -\left(M_{\text{a}} + Y_{\text{d}} \cdot a_4 \cdot \cos\phi_4 - X_{\text{d}} \cdot a_4 \cdot \sin\phi_4\right).$$

M_{a} [N-m] is the driving torque, from here on denoted as M_{drv}.

3.2 Optimization variables

In order to reduce the dynamic reactions, counterweights are added to each link. The counterweights' mass parameters, indicated with an asterisk $(\cdot)^*$, constitute the optimization variables, and are grouped into the optimization variable $\mathbf{x} \in \mathbb{R}^{12}$:

$$\mathbf{x} = \begin{bmatrix} m_1^* & X_1^* & Y_1^* & J_1^* & m_2^* & X_2^* & Y_2^* & J_2^* & m_3^* & X_3^* & Y_3^* & J_3^* \end{bmatrix}^T.$$

m_{i} [kg] and J_{i} [kg-m^2] respectively denote the mass and centroidal moment of inertia of the i-th link. For each link, the counterweight's center of gravity (COG) coordinates X_{i}^* [m] and Y_{i}^* [m] are defined with respect to the corresponding link coordinate system, defined in Fig.1(a).

3.3 Goal function

For calculating the goal function, the dynamic reactions are sampled at N equidistant points in one period T. In this way, $\mathbf{F}_{\text{shak,x}} \in \mathbb{R}^N$ is defined as:

$$\mathbf{F}_{\text{shak,x}} = [F_{\text{shak,x}}(T_{\text{s}}) \quad \ldots \quad F_{\text{shak,x}}(N \cdot T_{\text{s}})]^T , \tag{1}$$

where $T_{\text{s}} = T/N$ [s] denotes the sample period. In a similar fashion, $\mathbf{F}_{\text{shak,y}}$, $\mathbf{F}_{\text{shak}}$, $\mathbf{M}_{\text{shak}}$ and $\mathbf{M}_{\text{drv}} \in \mathbb{R}^N$ are defined.

The *balancing effect index* α [-] is introduced in [3] as the $L2$-norm of the optimized dynamic reactions w.r.t. the norm of the original dynamic reactions, indicated with a superscript $(\cdot)^{\text{o}}$:

$$\begin{aligned}
\alpha_{\text{xy}} &= \|\mathbf{F}_{\text{shak}}\|/\|\mathbf{F}^{\text{o}}_{\text{shak}}\|;\\
\alpha_{\text{s}} &= \|\mathbf{M}_{\text{shak}}\|/\|\mathbf{M}^{\text{o}}_{\text{shak}}\|;\\
\alpha_{\text{d}} &= \|\mathbf{M}_{\text{drv}}\|/\|\mathbf{M}^{\text{o}}_{\text{drv}}\|.
\end{aligned}$$

A classical way of optimizing the dynamic reactions is to define the goal function as a weighted combination of the three balancing effect indices:

$$\text{minimize} \quad f_{\text{goal}} = W_{\text{xy}} \cdot \alpha_{\text{xy}} + W_{\text{s}} \cdot \alpha_{\text{s}} + W_{\text{d}} \cdot \alpha_{\text{d}},$$

where W_{xy}, W_{s} and W_{d} represent optimization weights. Here however, a different approach is adopted:

$$\begin{aligned}
&\text{minimize} && f_{\text{goal}} = \alpha_{\text{s}}, && \text{(3a)}\\
&\text{subject to} && \alpha_{\text{xy}} \leq \alpha^{\text{M}}_{\text{xy}}, && \text{(3b)}\\
& && \alpha_{\text{d}} \leq \alpha^{\text{M}}_{\text{d}}, && \text{(3c)}
\end{aligned}$$

that is, solely the shaking moment is minimized, while keeping the shaking force and driving torque under control using constraints on α_{xy} and α_{d}. $\alpha^{\text{M}}_{\text{xy}}$ and $\alpha^{\text{M}}_{\text{d}}$ represent upper bounds, chosen by the designer. This approach is inspired by [11, 4], and the general observation that M_{drv} is hard to reduce through counterweight addition. It therefore make sense to just constrain it, in order to keep it under control, instead of minimizing it.

3.4 Mass constraints

Besides the constraints (3b–3c), which keep α_{xy} and α_{d} under control, constraints are also required for the counterweights' mass parameters. Obviously, masses and moments of inertia must be positive. Moreover, bound constraints are required for the counterweight COG coordinates. Furthermore, the total, added mass is constrained to a maximum $m^{\text{M}}_{\text{tot}}$ [kg]. As a result, the following constraints are obtained, $i = \{1, 2, 3\}$:

$$\begin{aligned}
&m^*_{\text{i}} \geq 0; && \text{(4a)}\\
&J^*_{\text{i}} \geq 0; && \text{(4b)}\\
&X^{\text{m}}_{\text{i}} \leq X^*_{\text{i}} \leq X^{\text{M}}_{\text{i}}; && \text{(4c)}\\
&Y^{\text{m}}_{\text{i}} \leq Y^*_{\text{i}} \leq Y^{\text{M}}_{\text{i}}; && \text{(4d)}\\
&m^*_1 + m^*_2 + m^*_3 \leq m^{\text{M}}_{\text{tot}}. && \text{(4e)}
\end{aligned}$$

These constraints allow adding a nonzero mass with a zero inertia. Such a counterweight, in fact, is a *point mass*, which is theoretically, but not practically implementable.

3.5 Resulting optimization problem

The optimization problem with the optimization variable $\mathbf{x}$, (3a) as a goal function and the constraints (3b–3c) and (4a–4e) is nonconvex. This is due to the fact that the balancing effect indices α_{xy}, α_{s} and α_{d} are complicated, nonconvex functions of the optimization variable $\mathbf{x}$. The following section reveals how this nonconvex problem can be reformulated as a convex problem, more specifically, an SOCP.

4 Convex reformulation

Two 'tricks' are required for reformulating the optimization problem at hand as a convex optimization problem. Firstly, another mass parametrization is adopted, as shown in Section 4.1. The key element of this parametrization is that it has the property of superposition.

Secondly, the following result, well-known in both dynamic balancing, as in experimental robot identification, see e.g. [12, 13], is used: if given time trajectories are imposed to all degrees of freedom of an (open or closed) kinematic chain of rigid bodies, then a general dynamic reaction $f(t)$ can be expressed as:

$$f(t) = \mathbf{e}(t)^T \cdot \mathbf{p}, \tag{5}$$

where $\mathbf{e}(t) \in \mathbb{R}^n$ is a time-dependent vector, determined by the chain's kinematics, and $\mathbf{p} \in \mathbb{R}^n$ is a time-independent vector, of which the elements are functions of the link lengths and the mass parameters. This result is elaborated in Section 4.2. The results of Section 4.1 and 4.2 finally give rise to the SOCP proposed in Section 4.3.

4.1 Mass parametrization

Not the conventional mass parameters m_{i}, X_{i}, Y_{i} and J_{i} are used here, but the so-called μ-parameters:

$$\begin{aligned}
\mu_{1\mathrm{i}} &= m_{\mathrm{i}};\\
\mu_{2\mathrm{i}} &= m_{\mathrm{i}} \cdot X_{\mathrm{i}};\\
\mu_{3\mathrm{i}} &= m_{\mathrm{i}} \cdot Y_{\mathrm{i}};\\
\mu_{4\mathrm{i}} &= J_{\mathrm{i}} + m_{\mathrm{i}} \cdot \left(X_{\mathrm{i}}^2 + Y_{\mathrm{i}}^2\right).
\end{aligned}$$

These parameters are well-known in robotics literature, but are rather unknown in dynamic balancing literature. Seemingly, they are introduced for the first time in [14], in which also their remarkable superposition property is emphasized. That is, the overall μ-parameters of a link, after counterweight addition, equal the sum of the μ-parameters of the unbalanced link and the counterweight. The proof of the superposition property is trivial for $\mu_{1\mathrm{i}}, \mu_{2\mathrm{i}}$ and $\mu_{3\mathrm{i}}$ and based on Steiner's law for $\mu_{4\mathrm{i}}$. These proofs have been omitted for reasons of brevity. Grouping the μ-parameters of the original mechanism in $\boldsymbol{\mu}^{\mathrm{o}} \in \mathbb{R}^{12}$, the counterweight μ-parameters in $\boldsymbol{\mu}^{*} \in \mathbb{R}^{12}$ and the μ-parameters after counterweight addition in $\boldsymbol{\mu} \in \mathbb{R}^{12}$ yields:

$$\boldsymbol{\mu} = \boldsymbol{\mu}^{\mathrm{o}} + \boldsymbol{\mu}^{*}. \tag{7}$$

The constraints (4a–4e) are translated as follows to the μ-parameters, $i = \{1, 2, 3\}$:

$$\mu_{1\mathrm{i}}^* \geq 0; \tag{8a}$$

$$\mu_{1\mathrm{i}}^* \cdot \mu_{4\mathrm{i}}^* \geq \left(\mu_{2\mathrm{i}}^*\right)^2 + \left(\mu_{3\mathrm{i}}^*\right)^2; \tag{8b}$$

$$\mu_{1\mathrm{i}}^* \cdot X_{\mathrm{i}}^{\mathrm{m}} \leq \mu_{2\mathrm{i}}^* \leq \mu_{1\mathrm{i}}^* \cdot X_{\mathrm{i}}^{\mathrm{M}}; \tag{8c}$$

$$\mu_{1\mathrm{i}}^* \cdot Y_{\mathrm{i}}^{\mathrm{m}} \leq \mu_{3\mathrm{i}}^* \leq \mu_{1\mathrm{i}}^* \cdot Y_{\mathrm{i}}^{\mathrm{M}}; \tag{8d}$$

$$\mu_{11}^* + \mu_{12}^* + \mu_{13}^* \leq m_{\mathrm{tot}}^{\mathrm{M}}. \tag{8e}$$

All of these constraints are linear in the μ-parameters, except for (8b). In conjunction with the redundant constraint $\mu^*_{4\mathrm{i}} \geq 0$, (8a–8b) constitute a set of hyperbolic constraints, as they describe a half hyperboloid. Using the fact [10]:

$$\mathbf{w}^T\mathbf{w} \leq xy, x \geq 0, y \geq 0 \Longleftrightarrow \left\| \begin{bmatrix} 2\mathbf{w} \\ x-y \end{bmatrix} \right\| \leq x+y,$$

where $\mathbf{w}$ is a vector and x and y are scalars, (8a–8e) can be replaced by, $i = \{1,2,3\}$:

$$\left\| \begin{bmatrix} 2\mu^*_{2\mathrm{i}} \\ 2\mu^*_{3\mathrm{i}} \\ \mu^*_{1\mathrm{i}} - \mu^*_{4\mathrm{i}} \end{bmatrix} \right\| \leq \mu^*_{1\mathrm{i}} + \mu^*_{4\mathrm{i}}; \tag{9a}$$

$$\mu^*_{1\mathrm{i}} \cdot X^{\mathrm{m}}_{\mathrm{i}} \leq \mu^*_{2\mathrm{i}} \leq \mu^*_{1\mathrm{i}} \cdot X^{\mathrm{M}}_{\mathrm{i}}; \tag{9b}$$

$$\mu^*_{1\mathrm{i}} \cdot Y^{\mathrm{m}}_{\mathrm{i}} \leq \mu^*_{3\mathrm{i}} \leq \mu^*_{1\mathrm{i}} \cdot Y^{\mathrm{M}}_{\mathrm{i}}; \tag{9c}$$

$$\mu^*_{11} + \mu^*_{12} + \mu^*_{13} \leq m^{\mathrm{M}}_{\mathrm{tot}}. \tag{9d}$$

4.2 Linearly independent vectors

Given the kinematics of the four-bar mechanism, that is, the link lengths a_{i}, $i = \{1,2,3,4\}$, the fixed angle ϕ_4 and the time trajectory of $\phi_1(t)$, the following expressions for the dynamic reactions are obtained, see e.g. [1, 15]:

$$F_{\mathrm{shak,x}}(t) = \mathbf{e}^T_{\mathrm{x}}(t) \cdot \mathbf{p}_{\mathrm{xy}} = \sum_{i=1}^{4} e_{\mathrm{x,i}}(t) \cdot p_{\mathrm{xy,i}}; \tag{10a}$$

$$F_{\mathrm{shak,y}}(t) = \mathbf{e}^T_{\mathrm{y}}(t) \cdot \mathbf{p}_{\mathrm{xy}} = \sum_{i=1}^{4} e_{\mathrm{y,i}}(t) \cdot p_{\mathrm{xy,i}}; \tag{10b}$$

$$M_{\mathrm{shak}}(t) = \mathbf{e}^T_{\mathrm{s}}(t) \cdot \mathbf{p}_{\mathrm{s}} = \sum_{i=1}^{6} e_{\mathrm{s,i}}(t) \cdot p_{\mathrm{s,i}}; \tag{10c}$$

$$M_{\mathrm{drv}}(t) = \mathbf{e}^T_{\mathrm{d}}(t) \cdot \mathbf{p}_{\mathrm{d}} = \sum_{i=1}^{4} e_{\mathrm{d,i}}(t) \cdot p_{\mathrm{d,i}}. \tag{10d}$$

The functions $e_{\mathrm{x,i}}(t)$, $e_{\mathrm{y,i}}(t)$, $e_{\mathrm{s,i}}(t)$ and $e_{\mathrm{d,i}}(t)$ are determined by the mechanism's kinematics and are linearly independent. In dynamic balancing literature, these functions are known as *linearly independent vectors*, [1]. Appendix A derives expressions for them. Since $e_{\mathrm{s,1}}(t) = e_{\mathrm{d,1}}(t) = \ddot{\phi}_1(t)$, the first elements of $\mathbf{e}_{\mathrm{s}}(t)$ and $\mathbf{e}_{\mathrm{d}}(t)$ are zero, if the mechanism is driven with constant drive speed. In that case, the expressions for $M_{\mathrm{shak}}(t)$ and $M_{\mathrm{drv}}(t)$ respectively contain five (instead of six) and three (instead of four) nonzero terms, and hence the first element of $\mathbf{p}_{\mathrm{s}}$ and $\mathbf{p}_{\mathrm{d}}$ is dropped. Therefore, the notation $\mathbf{p}_{\mathrm{i}} \in \mathbb{R}^{n_{\mathrm{i}}}$, $i = \{xy, s, d\}$ is introduced, where

$$\begin{array}{ll} \{n_{\mathrm{xy}}, n_{\mathrm{s}}, n_{\mathrm{d}}\} = \{4,5,3\} & \text{(constant drive speed);} \\ \{n_{\mathrm{xy}}, n_{\mathrm{s}}, n_{\mathrm{d}}\} = \{4,6,4\} & \text{(fluctuating drive speed).} \end{array} \tag{11}$$

The time-independent elements of $\mathbf{p}_{\mathrm{i}}$, $i = \{xy, s, d\}$ are linear combinations of the μ-parameters:

$$p_{\mathrm{xy,1}} = \mu_{21} + a_1 \cdot \mu_{12} - \frac{a_1}{a_2} \cdot \mu_{22}; \tag{12a}$$

$$p_{\mathrm{xy,2}} = \mu_{31} - \frac{a_1}{a_2} \cdot \mu_{32}; \tag{12b}$$

$$p_{\mathrm{xy,3}} = \mu_{23} + \frac{a_3}{a_2} \cdot \mu_{22}; \tag{12c}$$

$$p_{\mathrm{xy,4}} = \mu_{33} + \frac{a_3}{a_2} \cdot \mu_{32}, \tag{12d}$$

and

$$p_{\text{s},1} = p_{\text{d},1} = \mu_{41} - \frac{2 \cdot a_1^2}{a_2} \cdot \mu_{22} + \mu_{12} \cdot a_1^2 + \frac{a_1^2}{a_2^2} \cdot \mu_{42}; \tag{13a}$$

$$p_{\text{s},2} = p_{\text{d},2} = \mu_{43} + \frac{a_3^2}{a_2^2} \cdot \mu_{42}; \tag{13b}$$

$$p_{\text{s},3} = p_{\text{d},3} = -\mu_{42} + a_2 \cdot \mu_{22}; \tag{13c}$$

$$p_{\text{s},4} = p_{\text{d},4} = \mu_{32}; \tag{13d}$$

$$p_{\text{s},5} = \mu_{23} + \frac{a_3}{a_2^2} \cdot \mu_{42}; \tag{13e}$$

$$p_{\text{s},6} = \mu_{33}. \tag{13f}$$

Starting from (10a–10d), it is shown in Appendix B that α_i is equal to $\|\mathbf{z}_\text{i}\|$, $i = \{xy, s, d\}$ where

$$\mathbf{z}_\text{i} = \mathbf{\Psi}_\text{i} \cdot \mathbf{p}_\text{i}, \tag{14}$$

and $\mathbf{z}_\text{i} \in \mathbb{R}^{n_\text{i}}$. The matrices $\mathbf{\Psi}_\text{i} \in \mathbb{R}^{n_\text{i} \times n_\text{i}}$ are determined by the kinematics of the four-bar. Expressions for these matrices are given in Appendix B.

4.3 Resulting SOCP

The optimization variable is defined as:

$$\mathbf{x} = \begin{bmatrix} (\boldsymbol{\mu}^*)^T & \boldsymbol{\mu}^T & \mathbf{p}_\text{xy}^T & \mathbf{p}_\text{s}^T & \mathbf{p}_\text{d}^T & \mathbf{z}_\text{xy}^T & \mathbf{z}_\text{s}^T & \mathbf{z}_\text{d}^T & q \end{bmatrix}^T,$$

where q is a scalar, auxiliary variable, the introduction of which is justified below. $\mathbf{x} \in \mathbb{R}^{49}$ if the input crank speed $\dot{\phi}_1$ is constant and $\mathbf{x} \in \mathbb{R}^{53}$ if it is fluctuating. The goal function to be minimized is:

$$f_\text{optim} = q.$$

Minimizing α_s (or equivalently $\|\mathbf{z}_\text{s}\|$) directly or minimizing q subject to $\|\mathbf{z}_\text{s}\| \leq q$ is equivalent. The auxiliary variable q has to be introduced in order to obtain a goal function, linear in the optimization variables. The minimum is to be sought subject to the following constraints:

1. linear equality constraints $\boldsymbol{\mu} = \boldsymbol{\mu}^\text{o} + \boldsymbol{\mu}^*$, due to the superposition of the original and counterweight μ-parameters;
2. linear equality constraints, due to the linear conversion (12a–12d,13a–13f) from $\boldsymbol{\mu}$ to $\mathbf{p}_\text{i}$, $i = \{xy, s, d\}$;
3. linear equality constraints, due to the linear conversion (14) from $\mathbf{p}_\text{i}$ to $\mathbf{z}_\text{i}$, $i = \{xy, s, d\}$;
4. linear inequality constraints (9b–9d) on the counterweight μ^*-parameters, $i = \{1, 2, 3\}$;
5. second-order cone constraints (9a) on the counterweight μ^*-parameters, $i = \{1, 2, 3\}$;
6. upper bounds (3b–3c) on the balancing indices α_xy and α_d. Since $\alpha_\text{i} = \|\mathbf{z}_\text{i}\|$, this is equivalent to imposing upper bounds on the norms of $\mathbf{z}_\text{i}$, $i = \{xy, d\}$, which gives rise to the following second-order cone constraints:
$$\|\mathbf{z}_\text{xy}\| \leq \alpha_\text{xy}^\text{M};$$
$$\|\mathbf{z}_\text{d}\| \leq \alpha_\text{d}^\text{M}.$$
7. an additional second-order cone constraint, due to the introduction of the auxiliary variable q:
$$\|\mathbf{z}_\text{s}\| \leq q.$$

This optimization problem has a linear goal function that is minimized subject to linear equality constraints, linear inequality constraints and second-order cone constraints. It is hence a second-order cone program. This convex program is equivalent to the original, nonconvex optimization problem.

	$i=1$	$i=2$	$i=3$
a_i [m]	0.0508	0.1524	0.0762
m_i [kg]	0.0894	0.2394	0.1215
X_i [m]	0.0254	0.0762	0.0381
Y_i [m]	0	0.102	0
J_i [10^{-3}kg-m^2]	0.0198	0.6792	0.2198

Table 1: Crank-rocker four-bar: numerical parameters of the three links. $a_4 = 0.1397$ m and ϕ_4 = 0.

5 Numerical results

The SOCP is applied to a four-bar linkage, also considered in [4, 5]. Table 1 defines the linkage parameters. The following values are adopted for the upper and lower bounds on the COG coordinates: $X_\mathrm{i}^\mathrm{m} = -a_\mathrm{i}/2$; $X_\mathrm{i}^\mathrm{M} = 3a_\mathrm{i}/2$; $Y_\mathrm{i}^\mathrm{m} = -a_\mathrm{i}/2$; $Y_\mathrm{i}^\mathrm{M} = a_\mathrm{i}/2$, $i = \{1, 2, 3\}$. Four different values of $m_\mathrm{tot}^\mathrm{M}$ are considered: $m_\mathrm{tot}^\mathrm{M} = \{0.112, 0.225, 0.337, 0.450\}$ kg, which respectively represent $\{25, 50, 75, 100\}$% of the original, total mechanism mass (0.45 kg). The main reason for constraining the total, added mass is to avoid excessive link loading.

41 equidistant values of $\alpha_\mathrm{xy}^\mathrm{M}$ between 0 and 1 are considered, and 25 equidistant values of $\alpha_\mathrm{d}^\mathrm{M}$ between 0.5 and 1.7. This implies that, for each of the four values of $m_\mathrm{tot}^\mathrm{M}$, the SOCP needs to be solved 1025 times, which, to give an idea of the great numerical efficiency, takes only about twenty minutes on a PentiumIII@600MHz processor. The optimization software used here is `SeDuMi`, a dedicated software package for solving optimization problems over symmetric cones [16].

In the obtained optima, the inequality constraint (9d) is always active, as well as all second-order cone constraints. This implies that (i) always the maximum amount of mass is added, (ii) with zero centroidal inertia (in other words: point masses are obtained) and (iii) $\alpha_\mathrm{xy} = \alpha_\mathrm{xy}^\mathrm{M}$ and $\alpha_\mathrm{d} = \alpha_\mathrm{d}^\mathrm{M}$.

Figure 2 shows contour plots of α_s as a function of $\alpha_\mathrm{xy} = \alpha_\mathrm{xy}^\mathrm{M}$ and $\alpha_\mathrm{d} = \alpha_\mathrm{d}^\mathrm{M}$, for the four selected values of $m_\mathrm{tot}^\mathrm{M}$. The crosses 'x' indicate infeasible points, which indicates that the required values of $\alpha_\mathrm{xy}^\mathrm{M}$ and $\alpha_\mathrm{d}^\mathrm{M}$ are too tight. Quite logically, the feasible area grows if the constraint on the total, added mass is relaxed (by increasing $m_\mathrm{tot}^\mathrm{M}$). The contour lines behave rather 'shaky' at the boundary of the feasible area: in this region, `SeDuMi` runs into numerical problems, and does not deliver reliable results.

Figure 2 proves that total shaking force balance ($\alpha_\mathrm{xy} = 0$) is not possible with the given mass constraints. It is however possible if the total, added mass is allowed to be an unrealistic 150% of the original mass. Zero driving torque is not possible either, but allowing for more added mass does not yield zero driving torque: only a massless four-bar can have zero input torque, as shown in e.g. [15].

Figure 2 provides an excellent tool for assessing the tradeoff between minimizing the shaking force, shaking moment and driving torque. It shows for instance that there do exist zones in which all of the three dynamic reactions are smaller than in the original mechanism ($\alpha_\mathrm{i} \leq 1$, $i = \{xy, s, d\}$). However, when the driving torque is allowed to be greater than in the original mechanism, the obtainable reductions for the other reactions are greater.

This is illustrated by Fig.3, which shows α_s as a function of $\alpha_\mathrm{xy}^\mathrm{M}$ if a 20% increase of the driving torque is allowed ($\alpha_\mathrm{d}^\mathrm{M} = 1.2$). If $m_\mathrm{tot}^\mathrm{M} = 0.112$ kg, both the shaking force and shaking moment can be reduced with nearly 20%. If $m_\mathrm{tot}^\mathrm{M}$ doubles or quadruples to 0.225 kg, respectively 0.450 kg, both reactions can be simultaneously reduced with approximately 30% or 40% respectively. This result suggests that the obtainable reduction is proportional to $\log(m_\mathrm{tot}^\mathrm{M})$. CWB is hence no magical solution: it is capable of decreasing the dynamic reactions, but at the cost of significant mass addition.

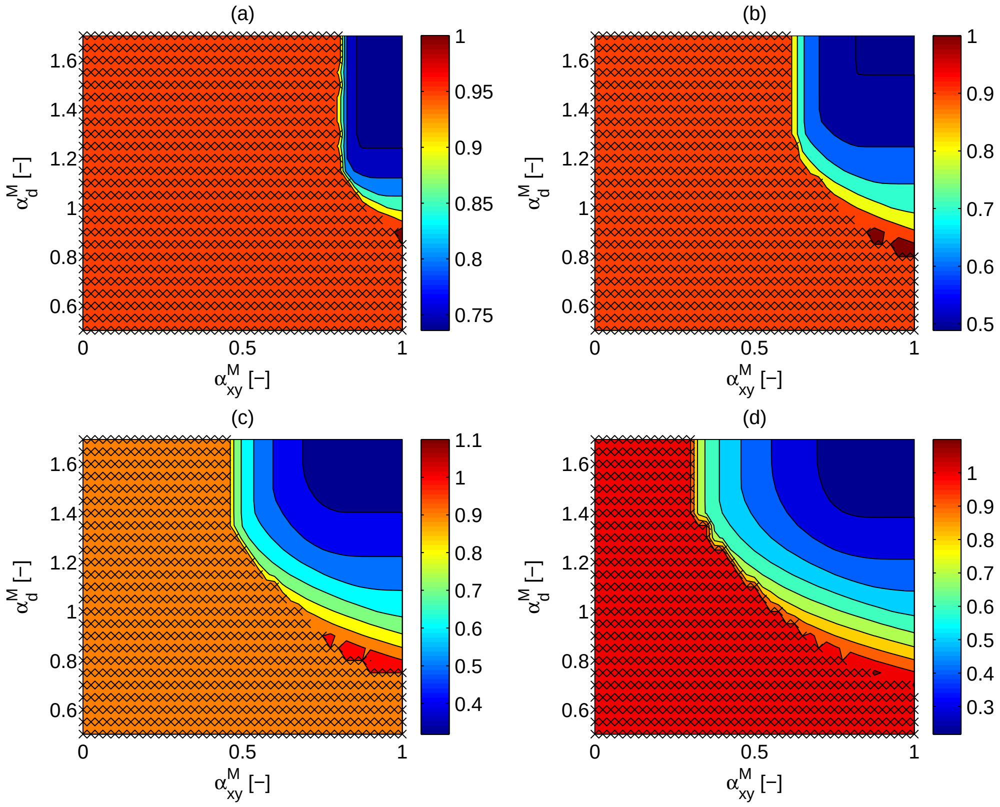

Figure 2: Contour plots of α_s [-] as a function of α_{xy}^M [-] and α_d^M [-] for m_{tot}^M equal to $\{0.112(a), 0.225(b), 0.337(c), 0.450(d)\}$ kg. the crosses 'x' indicate infeasible points.

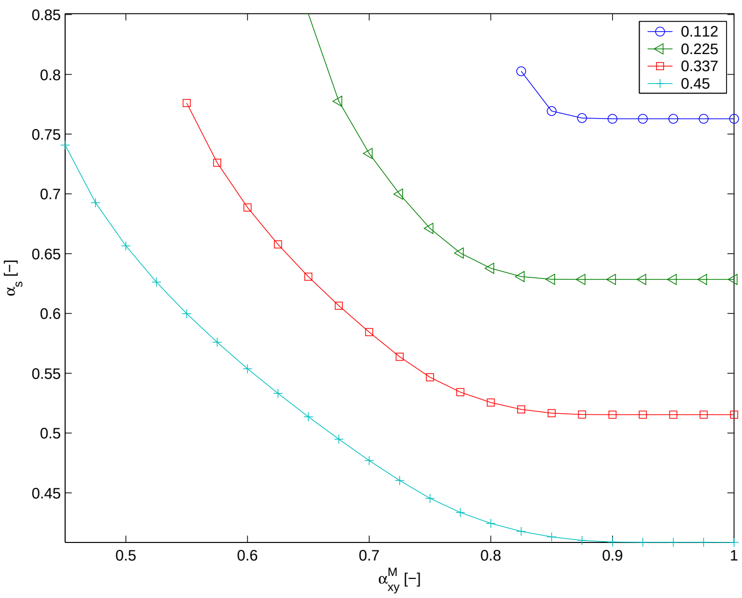

Figure 3: α_s [-] as a function of α_{xy}^M [-] for $\alpha_d^M = 1.2$ [-] and $m_{tot}^M = \{0.112, 0.225, 0.337, 0.450\}$ KG.

6 Discussion

It has been shown that counterweight balancing of plane, crank-rocker four-bars can be cast as a convex optimization problem, that is, an SOCP. Because of (i) the associated spectacular increase in computational efficiency, and (ii) the guarantee of obtaining a global optimum, it is possible to actually *prove* the obtained limits of dynamic balancing in a reasonable amount of time. The numerical results clearly illustrate (i) the tradeoff between minimizing the different dynamic reactions, and (ii) the fact that adding counterweights is effective, but at the cost of a significant amount of added mass.

The dynamic balancing limits obtained here are *ultimate* limits, in the sense that zero centroidal moment of inertia is allowed. Such point mass counterweights are not implementable in practice. The obtained results are however valuable in the sense that they provide an absolute reference with which practical counterweights should be compared. The obtained results may thus play the same role as does the theoretical Carnot-efficiency when assessing the efficiency of thermodynamic processes.

The developed method is not confined to four-bar linkages alone. It is applicable to any linkage, provided that linearly independent expressions such as (10a–10d) are available. For complicated planar mechanisms, developing such expressions is cumbersome. Automated procedures, implementable in computer programs, have however been proposed [17, 18]. Furthermore, the authors themselves have developed [19] a computer-aided, numerical method, on which they will report shortly.

When taking into account practical limits on counterweights, the constraint (9a) should be replaced by other types of constraints, of which the authors have proven [19] that they result in an SDP. Solving the numerical problems associated with this SDP and the SOCP at hand, is the subject of present and active research.

Acknowledgements

Bram Demeulenaere is a postdoctoral researcher with the Fund for Scientific Research–Flanders (Belgium) (F.W.O.). This work also benefits from K. U. Leuven's Concerted Research Action GOA/99/04. The scientific responsibility is assumed by its authors.

References

[1] R.S. Berkof and G.G. Lowen. A new method for completely force balancing simple linkages. *Transactions of the ASME, Journal of Engineering for Industry*, pages 21–26, 1969.

[2] G.G. Lowen, F.R. Tepper, and R.S. Berkof. Balancing of linkages–an update. *Mechanism and Machine Theory*, 18(3):213–220, 1983.

[3] G.G. Lowen, F.R. Tepper, and R.S. Berkof. The quantitative influence of complete force balancing on the forces and moments of certain families of four-bar linkages. *Mechanism and Machine Theory*, 9:299–323, 1974.

[4] S.J. Tricamo and G.G. Lowen. A novel method for prescribing the maximum shaking force of a four-bar linkage with flexibility in counterweight design. *Transactions of the ASME, Journal of Mechanisms, Transmissions, and Automation in Design*, 105:511–519, 1983.

[5] T.W. Lee and C. Cheng. Optimum balancing of combined shaking force, shaking moment, and torque fluctuations in high-speed linkages. *Transactions of the ASME, Journal of Mechanisms, Transmissions, and Automation in Design*, 106:242–251, 1984.

[6] R.T. Rockafellar. Lagrange multipliers and duality. *SIAM Review*, 35:183–283, 1993.

[7] S. Boyd and L. Vandenberghe. *Convex Optimization*. Cambridge University Press, 2004.

[8] G. Guo, N. Morita, and T. Torii. Optimum dynamic design of planar linkage using genetic algorithms. *JSME International Journal, Series C: Mechanical Systems, Machine Elements and Manufacturing*, 43(2):372–377, 2000.

[9] L. Vandenberghe and S. Boyd. Semidefinite programming. *SIAM Review*, 38(1):49–95, 1996.

[10] M.S. Lobo, L. Vandenberghe, S. Boyd, and H. Lebret. Applications of second-order cone programming. *Linear Algebra and its Applications*, 284(1–3):193–228, 1998.

[11] J.P. Sadler and R.W. Mayne. Balancing of mechanisms by nonlinear programming. *3rd Applied Mechanism Conference*, Paper No. 29, Oklahoma State University, Stillwater, Oklahoma, 1973.

[12] C.G. Atkeson, C.H. An, and J.M. Hollerbach. Estimation of inertial parameters of manipulator loads and links. *The International Journal of Robotics Research*, 5(3):101–119, 1986.

[13] J. Swevers, C. Ganseman, D. Tükel, J. De Schutter, and H. Van Brussel. Optimal robot excitation and identification. *IEEE Transactions on Robotics and Automation*, 13:730–739, 1997.

[14] R.S. Haines. Minimum rms shaking moment or driving torque of a force-balanced 4-bar linkage using feasible counterweights. *Mechanism and Machine Theory*, 16:185–190, 1981.

[15] J.L. Elliott and D. Tesar. The theory of torque, shaking force and shaking moment balancing of four link mechanisms. *Transactions of the ASME, Journal of Engineering for Industry*, pages 715–722, 1977.

[16] J.F. Sturm. Using sedumi 1.02, a matlab toolbox for optimization over symmetric cones. *Optimization Methods and Software*, 11–12:625–653, 1999. Special issue on Interior Point Methods (CD supplement with software).

[17] J.L. Elliott and D. Tesar. A general mass balancing method for complex planar mechanisms. *Mechanism and Machine Theory*, 17(2):153–172, 1982.

[18] I.S. Kochev. Contribution to the theory of torque, shaking force and shaking moment balancing of planar linkages. *Mechanism and Machine Theory*, 26(3):275–284, 1991.

[19] B. Demeulenaere. *Dynamic Balancing of Reciprocating Machinery With Application to Weaving Machines*. PhD thesis, Dept. of Mech. Eng., K.U.Leuven, Leuven, Belgium, 2004.

A Linearly independent vector expressions

(10a–10d) are obtained based on the following expressions:

$$F_{\text{shak,x}}(t) = -\mathrm{d}L_{\text{x}}/\mathrm{d}t; \tag{15a}$$
$$F_{\text{shak,y}}(t) = -\mathrm{d}L_{\text{y}}/\mathrm{d}t; \tag{15b}$$
$$M_{\text{shak}}(t) = -\mathrm{d}A/\mathrm{d}t; \tag{15c}$$
$$M_{\text{drv}}(t) = (\mathrm{d}E_{\text{kin}}/\mathrm{d}t)/\dot{\phi}_1(t). \tag{15d}$$

These expressions are valid provided that the four-bar mechanism is a kinematic chain of rigid bodies, in which no external work, gravity, friction nor springs are active. $L_{\text{x}}(t)$ [N-s] and $L_{\text{y}}(t)$ [N-s] denote the x and

y-component of the mechanism's linear momentum, whereas $A(t)$ [N-m-s] is its angular momentum w.r.t. the point a in Fig.1. $E_{\text{kin}}(t)$ [J] is the mechanism's kinetic energy. These quantities are given by:

$$L_{\text{x}} = \sum_{i=1}^{3} m_{\text{i}} \cdot \dot{r}_{\text{ix}}; \tag{16a}$$

$$L_{\text{y}} = \sum_{i=1}^{3} m_{\text{i}} \cdot \dot{r}_{\text{iy}}; \tag{16b}$$

$$A = \sum_{i=1}^{3} J_{\text{i}} \cdot \dot{\phi}_{\text{i}} + m_{\text{i}} \cdot \left(r_{\text{ix}} \cdot \dot{r}_{\text{iy}} - r_{\text{iy}} \cdot \dot{r}_{\text{ix}}\right); \tag{16c}$$

$$E_{\text{kin}} = \frac{1}{2} \cdot \sum_{i=1}^{3} J_{\text{i}} \cdot \dot{\phi}_{\text{i}}^2 + m_{\text{i}} \cdot \left(\dot{r}_{\text{ix}}^2 + \dot{r}_{\text{iy}}^2\right). \tag{16d}$$

r_{ix} [m] and r_{iy} [m] denote the x and y-component of the position (w.r.t to a) of link i's COG. Combining (16a–16d) with (15a–15d) yields (10a–10d) by (i) expressing r_{ix} and r_{iy} and their derivatives as a function of the link angles ϕ_{i}, $i = \{1, 2, 3\}$ and (ii) eliminating ϕ_2 and its derivatives, through application of the loop closure equations (and their time-derivatives):

$$a_1 \cdot c_1 + a_2 \cdot c_2 - a_3 \cdot c_3 - a_4 \cdot c_4 = 0;$$
$$a_1 \cdot s_1 + a_2 \cdot s_2 - a_3 \cdot s_3 - a_4 \cdot s_4 = 0,$$

where the shorthand notation $s_{\text{i}} = \sin \phi_{\text{i}}$; $c_{\text{i}} = \cos \phi_{\text{i}}$ is used. The functions that constitute the time-dependent elements of the vectors $\mathbf{e}_{\text{x}}(t)$, $\mathbf{e}_{\text{y}}(t)$, $\mathbf{e}_{\text{d}}(t)$ and $\mathbf{e}_{\text{s}}(t)$ in (10a–10d) are given by the following expressions, in which $s_{\text{ij}} = \sin\left(\phi_{\text{i}} - \phi_{\text{j}}\right)$ and $c_{\text{ij}} = \cos\left(\phi_{\text{i}} - \phi_{\text{j}}\right)$:

$$\begin{cases} e_{\text{x},1} = c_1 \cdot \dot{\phi}_1^2 + s_1 \cdot \ddot{\phi}_1; \\ e_{\text{x},2} = -s_1 \cdot \dot{\phi}_1^2 + c_1 \cdot \ddot{\phi}_1; \\ e_{\text{x},3} = c_3 \cdot \dot{\phi}_3^2 + s_3 \cdot \ddot{\phi}_3; \\ e_{\text{x},4} = -s_3 \cdot \dot{\phi}_3^2 + c_3 \cdot \ddot{\phi}_3; \end{cases} \qquad \begin{cases} e_{\text{y},1} = s_1 \cdot \dot{\phi}_1^2 - c_1 \cdot \ddot{\phi}_1; \\ e_{\text{y},2} = c_1 \cdot \dot{\phi}_1^2 + s_1 \cdot \ddot{\phi}_1; \\ e_{\text{y},3} = s_3 \cdot \dot{\phi}_3^2 - c_3 \cdot \ddot{\phi}_3; \\ e_{\text{y},4} = c_3 \cdot \dot{\phi}_3^2 + s_3 \cdot \ddot{\phi}_3; \end{cases}$$

$$\begin{cases} e_{\text{s},1} = -\ddot{\phi}_1; \\ e_{\text{s},2} = -\ddot{\phi}_3; \\ e_{\text{s},3} = \frac{a_1}{a_2^2} \cdot \Big\{ a_4 \cdot \left[s_{14} \cdot \dot{\phi}_1^2 - c_{14} \cdot \ddot{\phi}_1 \right] + \\ \qquad a_3 \cdot \left[s_{13} \cdot \left(\dot{\phi}_1^2 - \dot{\phi}_3^2 \right) - c_{13} \cdot \left(\ddot{\phi}_1 + \ddot{\phi}_3 \right) \right] \Big\}; \\ e_{\text{s},4} = \frac{a_1}{a_2} \cdot \Big\{ a_4 \cdot \left[-c_{14} \cdot \dot{\phi}_1^2 - s_{14} \cdot \ddot{\phi}_1 \right] + \\ \qquad a_3 \cdot \left[-c_{13} \cdot \left(\dot{\phi}_1^2 - \dot{\phi}_3^2 \right) - s_{13} \cdot \left(\ddot{\phi}_1 + \ddot{\phi}_3 \right) \right] \Big\}; \\ e_{\text{s},5} = a_4 \cdot \left[s_{34} \cdot \dot{\phi}_3^2 - c_{34} \cdot \ddot{\phi}_3 \right]; \\ e_{\text{s},6} = a_4 \cdot \left[c_{34} \cdot \dot{\phi}_3^2 + s_{34} \cdot \ddot{\phi}_3 \right]; \end{cases} \qquad \begin{cases} e_{\text{d},1} = \ddot{\phi}_1; \\ e_{\text{d},2} = \dot{\phi}_3 \cdot \ddot{\phi}_3 / \dot{\phi}_1; \\ e_{\text{d},3} = \frac{1}{\dot{\phi}_1} \cdot \frac{a_1 \cdot a_3}{a_2^2} \cdot \Big[-s_{13} \cdot \left(\dot{\phi}_1 - \dot{\phi}_3 \right) \cdot \dot{\phi}_1 \cdot \dot{\phi}_3 + \\ \qquad c_{13} \cdot \left(\ddot{\phi}_1 \cdot \dot{\phi}_3 + \dot{\phi}_1 \cdot \ddot{\phi}_3 \right) \Big]; \\ e_{\text{d},4} = \frac{1}{\dot{\phi}_1} \cdot \frac{a_1 \cdot a_3}{a_2} \cdot \Big[c_{13} \cdot \left(\dot{\phi}_1 - \dot{\phi}_3 \right) \cdot \dot{\phi}_1 \cdot \dot{\phi}_3 + \\ \qquad s_{13} \cdot \left(\ddot{\phi}_1 \cdot \dot{\phi}_3 + \dot{\phi}_1 \cdot \ddot{\phi}_3 \right) \Big]. \end{cases}$$

Combining (1) with (10a) shows that

$$\mathbf{F}_{\text{shak,x}} = \mathbf{E}_{\text{x}} \cdot \mathbf{p}_{\text{xy}}, \tag{17}$$

where $\mathbf{E}_{\text{x}} \in \mathbb{R}^{N \times n_{\text{xy}}}$ only depends on the mechanism's kinematics and is given by

$$\mathbf{E}_{\text{x}} = \left[\mathbf{e}_{\text{x}}(T_{\text{s}}) \quad \mathbf{e}_{\text{x}}(2T_{\text{s}}) \quad \ldots \quad \mathbf{e}_{\text{x}}(N \cdot T_{\text{s}}) \right]^T.$$

In a similar fashion, $\mathbf{E}_{\text{y}} \in \mathbb{R}^{N \times n_{\text{xy}}}$, $\mathbf{E}_{\text{s}} \in \mathbb{R}^{N \times n_{\text{s}}}$ and $\mathbf{E}_{\text{d}} \in \mathbb{R}^{N \times n_{\text{d}}}$ are obtained. Because of the elimination of ϕ_2 and its derivatives, the matrices $\mathbf{E}_{\text{x}}$, $\mathbf{E}_{\text{y}}$, $\mathbf{E}_{\text{s}}$ and $\mathbf{E}_{\text{d}}$ are of full rank.

B Balancing effect index expressions

Consider a vector $\mathbf{F} \in \mathbb{R}^N$, equal to, as in (17):

$$\mathbf{F} = \mathbf{E} \cdot \mathbf{p},$$

where $\mathbf{E} \in \mathbb{R}^{N\times n}$ is of full rank n. Its norm with respect to some reference norm $\|\mathbf{F}^{\mathrm{o}}\|$ (that is, the balancing effect index) then equals

$$\alpha = \frac{\|\mathbf{F}\|}{\|\mathbf{F}^{\mathrm{o}}\|} = \frac{\left(\mathbf{p}^T \cdot \mathbf{E}^T \cdot \mathbf{E} \cdot \mathbf{p}\right)^{\frac{1}{2}}}{\|\mathbf{F}^{\mathrm{o}}\|},$$

where $\mathbf{E}^T \cdot \mathbf{E}$ is symmetric and positive definite. Hence, its singular value decomposition equals

$$\mathbf{E}^T \cdot \mathbf{E} = \mathbf{U} \cdot \mathrm{diag}(\sigma_1, \ldots, \sigma_{\mathrm{n}}) \cdot \mathbf{U}^T,$$

where all singular values $\sigma_{\mathrm{j}} \geq 0$ and $\mathbf{U} \in \mathbb{R}^{n\times n}$. Defining $\mathbf{z}$ as:

$$\mathbf{z} = \frac{\mathrm{diag}(\sqrt{\sigma_1}, \ldots, \sqrt{\sigma_{\mathrm{n}}}) \cdot \mathbf{U}^T}{\|\mathbf{F}^{\mathrm{o}}\|} \cdot \mathbf{p} = \mathbf{\Psi} \cdot \mathbf{p},$$

where $\mathbf{z} \in \mathbb{R}^n$ and $\mathbf{\Psi} \in \mathbb{R}^{n\times n}$, we obtain:

$$\alpha = \|\mathbf{z}\|.$$

Based on this result, we have:

$$\begin{aligned}
\alpha_{\mathrm{xy}} &= \|\mathbf{z}_{\mathrm{xy}}\|;\\
\alpha_{\mathrm{s}} &= \|\mathbf{z}_{\mathrm{s}}\|;\\
\alpha_{\mathrm{d}} &= \|\mathbf{z}_{\mathrm{d}}\|,
\end{aligned}$$

where $\mathbf{z}_{\mathrm{i}} \in \mathbb{R}^{n_{\mathrm{i}}}$, $i = \{xy, s, d\}$, and

$$\begin{aligned}
\mathbf{z}_{\mathrm{xy}} &= \frac{\mathrm{diag}(\sqrt{\sigma_{\mathrm{xy},1}}, \ldots, \sqrt{\sigma_{\mathrm{xy},n_{\mathrm{xy}}}}) \cdot \mathbf{U}_{\mathrm{xy}}^T}{\|\mathbf{F}_{\mathrm{shak}}^{\mathrm{o}}\|} \cdot \mathbf{p}_{\mathrm{xy}} = \mathbf{\Psi}_{\mathrm{xy}} \cdot \mathbf{p}_{\mathrm{xy}};\\
\mathbf{z}_{\mathrm{s}} &= \frac{\mathrm{diag}(\sqrt{\sigma_{\mathrm{s},1}}, \ldots, \sqrt{\sigma_{\mathrm{s},n_{\mathrm{s}}}}) \cdot \mathbf{U}_{\mathrm{s}}^T}{\|\mathbf{M}_{\mathrm{shak}}^{\mathrm{o}}\|} \cdot \mathbf{p}_{\mathrm{s}} = \mathbf{\Psi}_{\mathrm{s}} \cdot \mathbf{p}_{\mathrm{s}};\\
\mathbf{z}_{\mathrm{d}} &= \frac{\mathrm{diag}(\sqrt{\sigma_{\mathrm{d},1}}, \ldots, \sqrt{\sigma_{\mathrm{d},n_{\mathrm{d}}}}) \cdot \mathbf{U}_{\mathrm{d}}^T}{\|\mathbf{M}_{\mathrm{drv}}^{\mathrm{o}}\|} \cdot \mathbf{p}_{\mathrm{d}} = \mathbf{\Psi}_{\mathrm{d}} \cdot \mathbf{p}_{\mathrm{d}}.
\end{aligned}$$

$\mathbf{U}_{\mathrm{i}} \in \mathbb{R}^{n_{\mathrm{i}}\times n_{\mathrm{i}}}$, $i = \{xy, s, d\}$ are determined based on:

$$\begin{aligned}
\mathbf{E}_{\mathrm{x}}^T \cdot \mathbf{E}_{\mathrm{x}} + \mathbf{E}_{\mathrm{y}}^T \cdot \mathbf{E}_{\mathrm{y}} &= \mathbf{U}_{\mathrm{xy}} \cdot \mathrm{diag}(\sigma_{\mathrm{xy},1}, \ldots, \sigma_{\mathrm{xy},n_{\mathrm{xy}}}) \cdot \mathbf{U}_{\mathrm{xy}}^T;\\
\mathbf{E}_{\mathrm{s}}^T \cdot \mathbf{E}_{\mathrm{s}} &= \mathbf{U}_{\mathrm{s}} \cdot \mathrm{diag}(\sigma_{\mathrm{s},1}, \ldots, \sigma_{\mathrm{s},n_{\mathrm{s}}}) \cdot \mathbf{U}_{\mathrm{s}}^T;\\
\mathbf{E}_{\mathrm{d}}^T \cdot \mathbf{E}_{\mathrm{d}} &= \mathbf{U}_{\mathrm{d}} \cdot \mathrm{diag}(\sigma_{\mathrm{d},1}, \ldots, \sigma_{\mathrm{d},n_{\mathrm{d}}}) \cdot \mathbf{U}_{\mathrm{d}}^T.
\end{aligned}$$